Electronic Supplementary Material (ESI) for Biomaterials Science.


Electric Supplementary Information

# Stretch-Responsive Adhesive Microcapsules for Strain-Regulated Antibiotic Release from Fabric Wound Dressings

*Yun Kee Jo, Su-Jin Heo, Ana P. Peredo, Robert L. Mauck*, George R. Dodge* and Daeyeon Lee**

*E-mail: daeyeon@seas.upenn.edu

**Table S1.** Adhesion strength of PDA-MAMCs at different concentration of PDA coating to porcine skin and a plastic surface ($n \geq 4$).

| Substrate | 1 mg/ml PDA | 10 mg/ml PDA |
|---|---|---|
| Porcine skin | 633 ± 106 g | 689 ± 93 g |
| Plastic | 510 ± 77 g | 608 ± 109g |

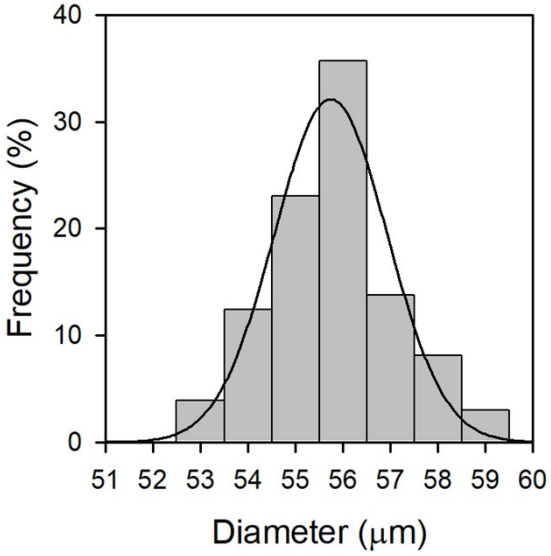


**Fig. S1** Size distribution of MAMCs.

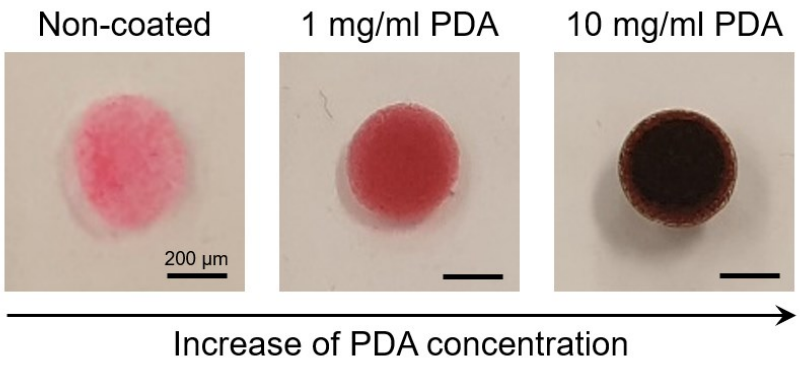


**Fig. S2** Optimal images of MAMCs before and after PDA coating. The brown color becomes darker with the increase of the concentration of PDA.

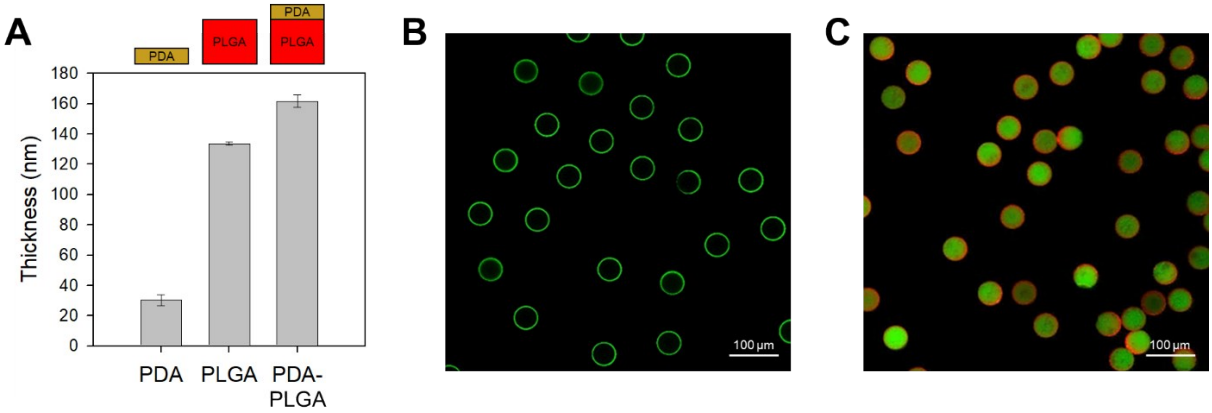


**Fig. S3** (A) Thickness of PDA coating layer, PLGA film and PDA-coated PLGA film measured by ellipsometry. (B) Confocal microscopy image of the PDA-MAMCs with labeled PDA coating layer (green). To clearly visualize the PDA layer, non-labeled BSA is used as the aqueous core. (C) Confocal microscopy image of the PDA-MAMCs with labeled PLGA shells (red) used for mechano-activation analyses (% Full > 95). To accurately quantify the percentage of full microcapsules, fluorescent BSA (green) is encapsulated into the PDA-MAMC with non-labeled PDA coating layer.

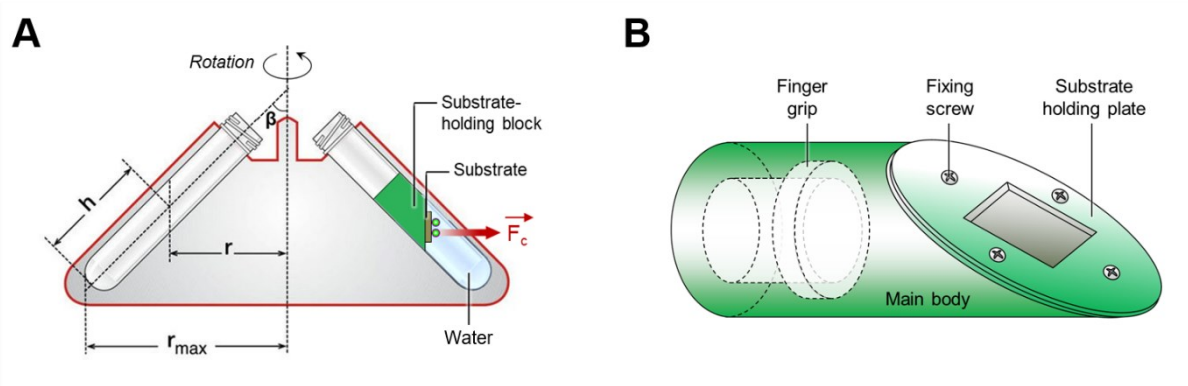


**Fig. S4** Measurement of adhesion strength of PDA-MAMCs. Schematic illustration of (A) the centrifuge method for measurement of adhesion strength and (B) the custom-designed substrate-holding block. β, the angle of the centrifuge tube; h, the height of sample in the centrifuge tube; r, the radial diameter of the samples; $r_{max}$, the maximum radial diameter of the centrifuge tube.

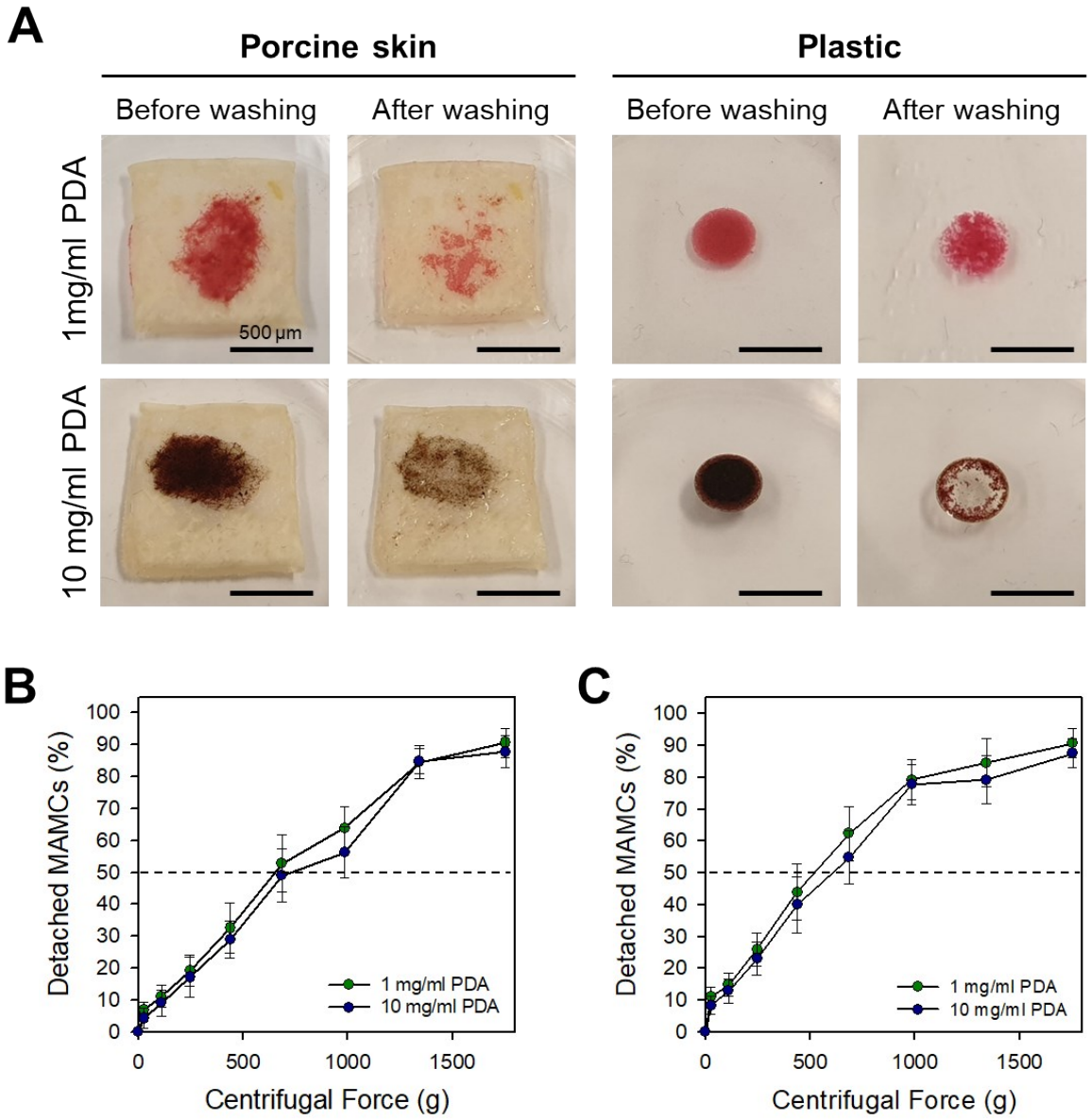


**Fig. S5** Adhesiveness of PDA-MAMCs at different concentration of PDA coating. (A) Images showing adhesion of microcapsules to porcine skin and a plastic surface. (B, C) Microcapsule detachment profiles from (B) porcine skin and (C) a plastic surface as a function of centrifugal force ($n \geq 4$ specimens, ***$p<0.005$, **$p<0.01$, *$p<0.05$; Kolmogorov-Smirnov test).

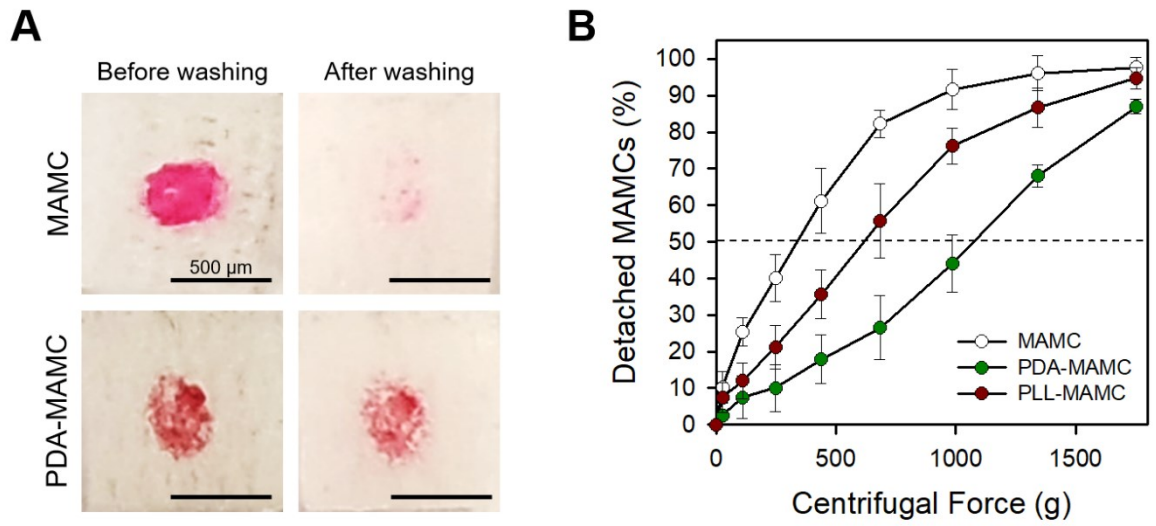


**Fig. S6** Adhesion of PDA-MAMCs on the fabric dressing. (A) Images showing adhesion of MAMCs and PDA-MAMCs on a gauze. (B) Microcapsule detachment profiles from the gauze at different centrifugal forces ($n \geq 4$ specimens; ***$p<0.005$, **$p<0.01$, *$p<0.05$; Kolmogorov-Smirnov test).

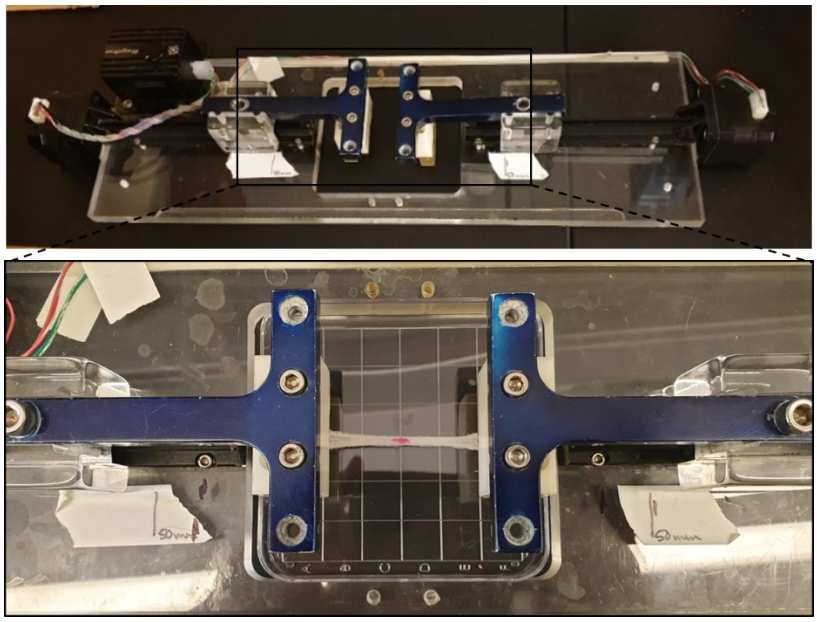

**Fig. S7** Experimental setup of a custom-built micromechanical tester.

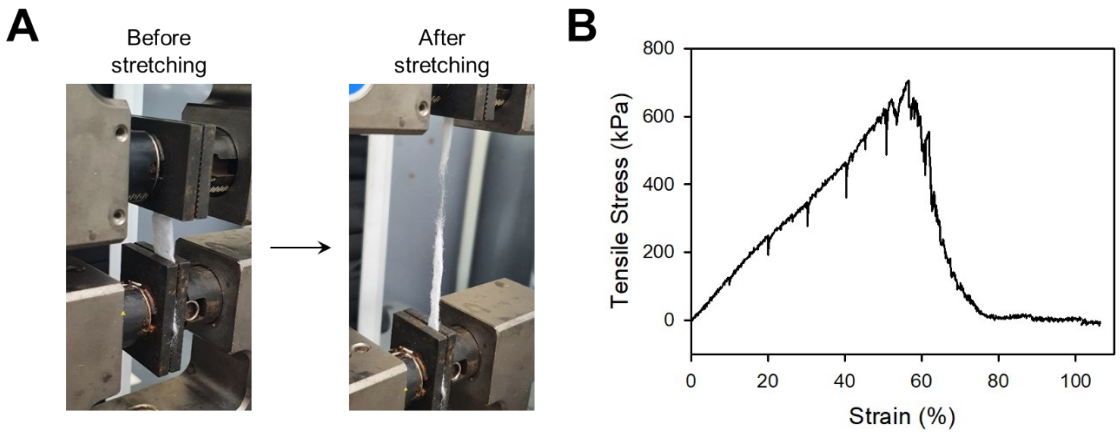


**Fig. S8** (A) Photographs of a gauze before and after application of tensile strain. (B) Strain–stress curve of the gauze upon uniaxial stretching with 10% stepwise increments at a strain rate of 1%/s.

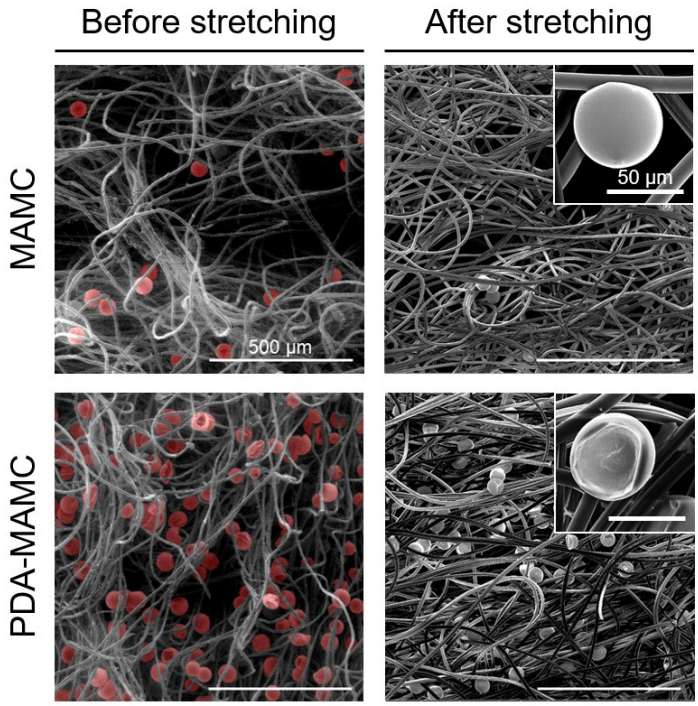


**Fig. S9** Stretch-induced mechano-activation of PDA-MAMCs in the fibrous matrix of gauze. SEM images of the gauze loaded with pseudo-red-colored microcapsules before and after stretching.

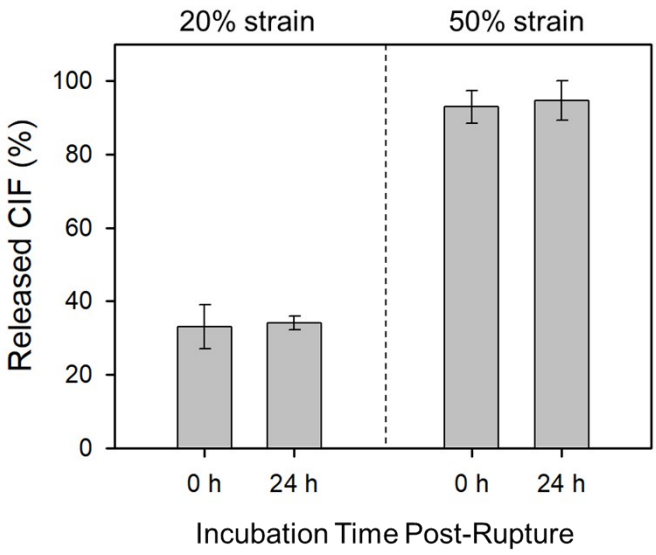


**Fig. S10** Released CIF from the CIF@PDA-MAMCs-laden gauze immediately (0 h) after or 24 h after rupture induced by stretching with tensile strains of 20% and 50% ($n \geq 500$ microcapsules/loading regimen/type, 4 specimens/loading regimen/type).